ality of epitope presentation as the key factor in the rapid and selective differentiation of cells into neurons. An average-sized nanofiber in the network contains an estimated 7.1×10^{14} IKVAV epitopes/cm^2. By contrast, closely packed laminin protein molecules in a two-dimensional lattice on a solid substrate have an estimated 7.5×10^{11} IKVAV epitopes/cm^2 (*22*). Thus, the IKVAV nanofibers of the network could amplify the epitope density relative to a laminin monolayer by roughly a factor of 10^3 (*22*).

The self-assembly of the scaffold studied here can also be triggered by injection of peptide amphiphile solutions into tissue. We injected 10 to 80 μl of 1 wt % peptide amphiphile solutions into freshly enucleated rat eye preparations and in vivo into rat spinal cords following a laminectomy to expose the cord (*22*). Thus, these peptide amphiphile solutions can indeed be transformed into a solid scaffold upon contact with tissues. This process localizes the network in tissue and prevents passive diffusion of the molecules away from the epicenter of an injection site. Furthermore, it is known that animals survive for prolonged periods after injections of the peptide amphiphile solutions into the spinal cord, a finding of relevance to the present study.

References and Notes

1. R. Langer, J. P. Vacanti, *Science* **260**, 920 (1993).
2. A. Lendlein, R. Langer, *Science* **296**, 1673 (2002).
3. Y. D. Teng *et al*., *Proc. Natl. Acad. Sci. U.S.A.* **99**, 3024 (2002).
4. L. Lu *et al*., *Biomaterials* **21**, 1837 (2000).
5. L. E. Niklason., *Science* **284**, 489 (1999).
6. S. Nehrer *et al*., *J. Biomed. Mater. Res.* **38**, 95 (1997).
7. A. Atala *et al*., *J. Urol.* **150**, 745 (1993).
8. H. L. Wald *et al*., *Biomaterials* **14**, 270 (1993).
9. I. V. Yannas, J. F. Burke, D. P. Orgill, E. M. Skrabut, *Science* **215**, 174 (1982).
10. D. J. Mooney *et al*., *Biomaterials* **17**, 1417 (1996).
11. A. G. Mikos, M. D. Lyman, L. E. Freed, R. Langer, *Biomaterials* **15**, 55 (1994).
12. E. Lavik, Y. D. Teng, E. Snyder, R. Langer, *Methods Mol. Biol*. **198**, 89 (2002).
13. W. C. Hsu, M. H. Spilker, I. V. Yannas, P. A. Rubin, *Invest. Ophthalmol. Vis. Sci.* **41**, 2404 (2000).
14. L. J. Chamberlain, I. V. Yannas, H. P. Hsu, G. R. Strichartz, M. Spector, *J. Neurosci. Res.* **60**, 666 (2000).
15. C. E. Butler, I. V. Yannas, C. C. Compton, C. A. Correia, D. P. Orgill, *Br. J. Plast. Surg.* **52**, 127 (1999).
16. D. P. Orgill *et al*., *Plast. Reconstr. Surg.* **102**, 423 (1998).
17. S. C. Chang *et al*., *J. Biomed. Mater. Res.* **55**, 503 (2001).
18. A. Atala *et al*., *J. Urol.* **150**, 745 (1993).
19. F. Lim, A. M. Sun, *Science* **210**, 908 (1980).
20. G. Hortelano, A. Al-Hendy, F. A. Ofosu, P. L. Chang, *Blood* **87**, 5095 (1996).
21. W. Xu, L. Liu, I. G. Charles, *FASEB J.* **16**, 213 (2002).
22. Materials and methods are available as supporting material on *Science* Online.
23. H. Okano, *J. Neurosci. Res.* **69**, 698 (2002).
24. A. Storch, J. Schwarz, *Curr. Opin. Invest. Drugs* **3**, 774 (2002).
25. M. F. Mehler, J. A. Kessler, *Arch. Neurol.* **56**, 780 (1999).
26. D. W. Pincus, R. R. Goodman, R. A. Fraser, M. Nedergaard, S. A. Goldman, *Neurosurgery* **42**, 858 (1998).
27. L. Kam, W. Shain, J. N. Turner, R. Bizios, *Biomaterials* **22**, 1049 (2001).
28. M. Matsuzawa, F. F. Weight, R. S. Potember, P. Liesi, *Int. J. Dev. Neurosci.* **14**, 283 (1996).
29. S. K. Powell *et al*., *J. Neurosci. Res.* **61**, 302 (2000).
30. T. Cornish, D. W. Branch, B. C. Wheeler, J. T. Campanelli, *Mol. Cell. Neurosci.* **20**, 140 (2002).
31. J. C. Chang, G. J. Brewer, B. C. Wheeler, *Biosens. Bioelectron.* **16**, 527 (2001).
32. B. C. Wheeler, J. M. Corey, G. J. Brewer, D. W. Branch, *J. Biomech. Eng.* **121**, 73 (1999).
33. L. Lauer, A. Vogt, C. K. Yeung, W. Knoll, A. Offenhausser, *Biomaterials* **23**, 3123 (2002).
34. P. Thiebaud, L. Lauer, W. Knoll, A. Offenhausser, *Biosens. Bioelectron.* **17**, 87 (2002).
35. C. K. Yeung, L. Lauer, A. Offenhausser, W. Knoll, *Neurosci. Lett.* **301**, 147 (2001).
36. The EQS peptide sequence has no known physiological signaling function but has a charge distribution that allows nanofiber self-assembly.
37. J. D. Hartgerink, E. Beniash, S. I. Stupp, *Science* **294**, 1684 (2001).
38. J. D. Hartgerink, E. Beniash, S. I. Stupp, *Proc. Natl. Acad. Sci. U.S.A.* **99**, 5133 (2002).
39. In vitro self-assembly was induced by addition of Dulbecco's minimum essential medium (DMEM), DMEM/F12, and modifications thereof, as well as by addition of cerebral spinal fluid.
40. Cell viability and toxicity was assessed using Molecular Probes Live/Dead assay (*22*).
41. G. A. Silva *et al*., data not shown.
42. G. Zhu, M. F. Mehler, P. C. Mabie, J. A. Kessler, *J. Neurosci. Res.* **59**, 312 (2000).
43. A. G. Rabchevsky, G. M. Smith, *Arch. Neurol.* **58**, 721 (2001).
44. Z. J. Chen, Y. Ughrin, J. M. Levine, *Mol. Cell. Neurosci.* **20**, 125 (2002).
45. S. Costa *et al*., *Glia* **37**, 105 (2002).
46. F. H. Gage, J. Ray, L. J. Fisher, *Annu. Rev. Neurosci.* **18**, 159 (1995).
47. M. Parmar, C. Skogh, A. Bjorklund, K. Campbell, *Mol. Cell. Neurosci.* **21**, 645 (2002).
48. S. Wu *et al*., *J. Neurosci. Res.* **72**, 343 (2003).
49. E. Alsberg, K. W. Anderson, A. Albeiruti, J. A. Rowley, D. J. Mooney, *Proc. Natl. Acad. Sci. U.S.A.* **99**, 12025 (2002).
50. L. Canaple, A. Rehor, D. Hunkeler, *J. Biomater. Sci. Polym. Ed.* **13**, 783 (2002).
51. S. C. Chang *et al*., *J. Biomed. Mater. Res.* **55**, 503 (2001).
52. J. J. Marler *et al*., *Plast. Reconstr. Surg.* **105**, 2049 (2000).
53. J. A. Rowley, D. J. Mooney, *J. Biomed. Mater. Res.* **60**, 217 (2002).

54. For 2D IKVAV-PA cell experiments, we first coated cover slips with PDL to ensure that the negatively charged IKVAV-PA nanofibers would adhere to the surface, and then placed 300 ml of 1 wt % aqueous solutions of the PA on surfaces and allowed them to dry overnight in a fume hood. We prepared the IKVAV peptide cover slips by spin-coating the peptide on the surface. The next day, all coated plates were washed three times with distilled water to remove any material not strongly adsorbed to the surface.

55. This material is based on work supported by the U.S. Department of Energy (grant DE-FG02-00ER45810/A001), NIH (grants NS20778, NS20013, and NS34758), and NSF (DMR-010-8342). Any opinions, findings, and conclusions or recommendations expressed in this work are those of the authors and do not necessarily reflect the views of these agencies.

Supporting Online Material

www.sciencemag.org/cgi/content/full/1093783/DC1
Materials and Methods
Fig. S1
References and Notes

18 November 2003; accepted 13 January 2004
Published online 22 January 2004;
10.1126/science.1093783
Include this information when citing this paper.

Carbon and Nitrogen Isotopic Anomalies in an Anhydrous Interplanetary Dust Particle

Christine Floss,[1]* Frank J. Stadermann,[1] John Bradley,[2] Zu Rong Dai,[2] Saša Bajt,[2] Giles Graham[2]

Because hydrogen and nitrogen isotopic anomalies in interplanetary dust particles have been associated with carbonaceous material, the lack of similar anomalies in carbon has been a major conundrum. We report here the presence of a ^{13}C depletion associated with a ^{15}N enrichment in an anhydrous interplanetary dust particle. Our observations suggest that the anomalies are carried by heteroatomic organic compounds. Theoretical models indicate that low-temperature formation of organic compounds in cold interstellar molecular clouds can produce carbon and nitrogen fractionations, but it remains to be seen whether the specific effects observed here can be reproduced.

Interstellar molecular clouds are the principal formation sites of organic matter in the Milky Way galaxy. A variety of simple molecules, such as CH_4, CH_3OH, and H_2CO, are produced in dense cold (10 to 30 K) clouds (*1*). At such low temperatures, where the difference in chemical binding energy exceeds thermal energy, mass fractionation produces molecules with isotopic ratios that can be anomalous relative to terrestrial values (*1–3*). Such anomalous ratios potentially provide a fingerprint for abiotic interstellar organic matter that was incorporated into the solar system and survives today in cosmically primitive materials such as interplanetary dust particles (IDPs).

IDPs collected in Earth's stratosphere are complex assemblages of primitive solar system material and carry various isotopic

[1]Laboratory for Space Sciences, Washington University, St. Louis, MO 63130, USA. [2]Institute for Geophysics and Planetary Physics, Lawrence Livermore National Laboratory, Livermore, CA 94550, USA.

*To whom correspondence should be addressed. E-mail: floss@wustl.edu

anomalies (*2*, *4*, *5*). Deuterium enhancements result from extreme chemical fractionation in cold molecular clouds (*6*), and D/H ratios in some IDPs approach the values observed in interstellar molecules (*7*), suggesting the intact survival of some molecular cloud material. Nitrogen isotopic anomalies, in the form of ^{15}N enrichments, are also common and are postulated to result from low-temperature interstellar chemistry (*2*, *8*). This origin is complicated because N isotopic fractionation has not been observed in the interstellar medium and because anomalous N can also have a nucleosynthetic origin. However, recent work shows that chemical reactions in dense molecular gases can produce elevated $^{15}N/^{14}N$ ratios (*9*, *10*), although the maximum enhancements fall short of observed ^{15}N enrichments in IDPs (*11*, *12*). Organic compounds appear to be the source of many of the D and ^{15}N enrichments (*13*–*15*); it is puzzling, therefore, that C isotopic anomalies have not been observed, despite numerous measurements (*5*).

We carried out simultaneous C and N isotopic imaging measurements of an anhydrous noncluster particle (L2036-G16), using the NanoSIMS, a new generation secondary ion mass spectrometer that allows isotopic imaging at a spatial scale of 100 nm. The particle, nicknamed Benavente (*16*), was pressed into a high-purity Au substrate along with isotopic standards, which were measured together with the IDP on the same sample mount (*17*). The bulk C isotopic composition of Benavente is normal, with a $^{12}C/^{13}C$ ratio of 89.3 ± 1.0 ($\delta^{13}C$ = +8 ± 11‰), but the IDP is enriched in ^{15}N, with an average $^{14}N/^{15}N$ ratio of 224.3 ± 1.7 ($\delta^{15}N$ = +213 ± 9‰). Benavente also contains a large (0.6 × 1.8 μm^2) region that is strongly enriched in ^{15}N ($^{14}N/^{15}N$ = 119.8 ± 1.3; $\delta^{15}N$ = +1270 ± 25‰) and depleted in ^{13}C ($^{12}C/^{13}C$ = 96.6 ± 1.3; $\delta^{13}C$ = –70 ± 13‰) (Fig. 1) (*18*). Although the ^{13}C depletion is not great, its importance is emphasized by the large size of the region and its association with the ^{15}N enrichment (Fig. 2) (*19*). Furthermore, both anomalies are consistently present in the 25 successively measured layers. Several studies (*20*–*22*) indicate a solar N isotopic composition that is ~30% lighter than the terrestrial one. Thus, the ^{15}N enrichments in Benavente relative to solar composition may be considerably higher than the values noted here. Moreover, recent work (*23*) suggests that solar C may be ~10% lighter than terrestrial C, a value that is similar to the magnitude of the ^{13}C depletion in our anomalous region.

In addition to isotopic information, our analysis provides clues to the nature of the carrier phase(s) of the C and N anomaly in Benavente. The anomalous region has a higher C^- yield than most of the IDP and a CN^-/C^- ratio of ~0.9, suggesting that the C and N anomalies are carried by organic matter. If this material is carbonaceous, the calibration curve of CN^-/C^- ratios versus N concentrations in organic material established by (*24*) suggests a N concentration of ~3.0 ± 1.5 weight % (wt %). This is at the upper end of the range of N concentrations of insoluble organic matter in carbonaceous chondrites (*15*) and falls within the field observed for CHON grains from comet Halley (*25*). Recent measurements of the $^{14}N/^{15}N$ ratios of the CN radical in the coma of two comets give a value of 140 ± 30 (*26*), within errors the same as that of the $^{14}N/^{15}N$ ratio of our anomalous region.

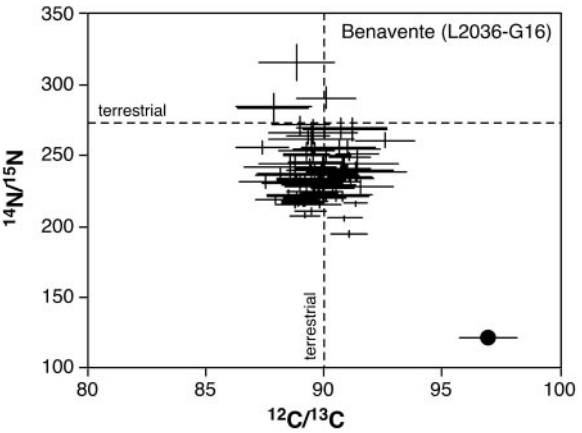

Fig. 1. Isotopic composition of the anomalous region compared with similar-sized areas of Benavente. Nitrogen isotopic compositions spread toward subterrestrial ratios in the "bulk" of the particle, indicating an overall enrichment in ^{15}N.

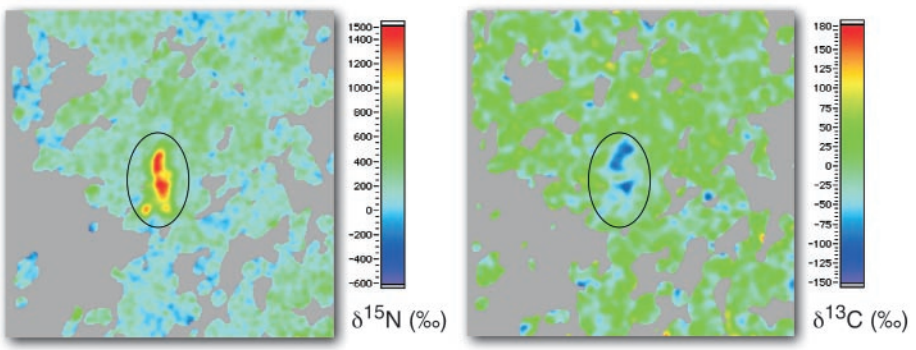

Fig. 2. $\delta^{15}N$ (**left**) and $\delta^{13}C$ (**right**) images of Benavente showing the ^{15}N-enriched and ^{13}C-depleted anomalous region. Field of view is 10 μm.

Using a focused ion beam (FIB) technique (*27*), we extracted a section (~5 by 1 by 0.1 μm) from an area about 5 μm from the anomalous region. This area has lower C^- and CN^- signals than the anomalous region, and C and N isotopic compositions similar to the bulk IDP. Using a transmission electron microscope (TEM), we employed energy-filtered imaging to investigate the mineralogy of the section (*17*). The region is rich in GEMS (glass with embedded metal and sulfides) (*28*) and also contains forsterite (Mg_2SiO_4), iron-rich sulfides (pyrrhotite, $Fe_{1-x}S$), and abundant amorphous carbonaceous material that is clumped into distinct regions and coats some grains, such as the GEMS.

After the TEM investigation, we mapped the C and N isotopic compositions in the FIB slice with the NanoSIMS and reconfirmed the ^{15}N enrichment of ~200 ‰ observed in the bulk IDP. Moreover, we found a 250-nm region with a strong ^{15}N enrichment of +1110 ± 98‰ that was not seen in the original NanoSIMS measurement because it is located below the original surface of the IDP. Spatial correlation of this anomaly with the TEM images (Fig. 3) shows that it consists of amorphous carbonaceous material immediately surrounded by GEMS and other silicates. Infrared (IR) spectra (*17*) show a prominent C-H stretch feature at ~3.4 μm (Fig. 4), similar to that observed in meteoritic kerogen (*4*). The positions of the bands within the feature are consistent with those of aliphatic hydrocarbons, confirming the organic nature of carbonaceous material. Aromatic hydrocarbons are likely to be present too, but are probably dominated by the strong resonance of the aliphatic C-H feature. Nitrogen abundances in the FIB section are low (1 to 2 wt %, based on electron energy loss spectroscopy), but the N is associated with the carbonaceous material and, thus, has an organic origin. No other elements are associated with the N

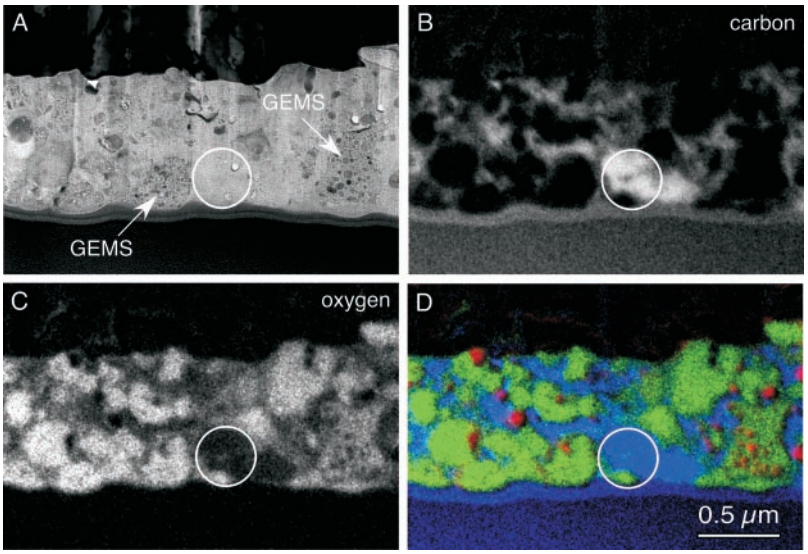

Fig. 3. FIB section extracted from Benavente showing, in the circle, the ^{15}N-rich region. (**A**) Bright-field TEM image (300 keV). GEMS, glass with embedded metal and sulfides. (**B**) Energy-filtered carbon jump-ratio image. (**C**) Energy-filtered oxygen jump-ratio image. (**D**) Composite image showing silicates (green), carbonaceous material (blue), and iron or iron sulfides (red).

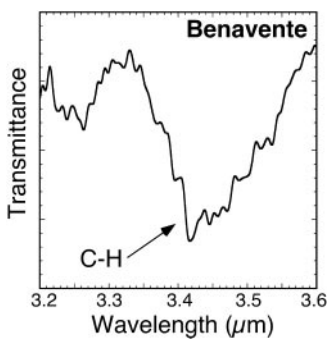

Fig. 4. IR spectrum of the Benavente FIB section, showing the C-H stretch feature at 3.4 μm indicative of hydrocarbons.

that might indicate the presence of a different carrier phase. The ^{15}N-rich region in the FIB slice is not ^{13}C-depleted (probably because of the small size of the area, leading to dilution effects from surrounding isotopically normal C), but the similarity of the magnitude of the N anomaly to that of the C- and N-anomalous region (and the proximity of the FIB slice to the original anomalous area) suggests that the same type of amorphous carbon is the carrier of the correlated C and N anomaly. Although presolar graphite in meteorites is ^{15}N-enriched and ^{13}C-depleted (*29*), it is unlikely to be the carrier phase of the C and N anomaly in Benavente: Our TEM and spectroscopic work shows that only amorphous carbon is present in this IDP. Moreover, in contrast to carbonaceous chondrites, graphitic carbon is conspicuously absent from chondritic IDPs (*4*, *30*).

Without C isotopic anomalies, it is not possible to distinguish whether the carbonaceous material in IDPs is itself presolar or simply a more "recent" (e.g., solar system) host substrate for presolar D and ^{15}N-enriched species. Previous studies have suggested that some IDPs contain carbon compounds with heteroatoms (e.g., N in –CN attached to aromatic chromophores) (*31*), but without correlated C and N isotopic data, the origin of such molecules has remained uncertain (*13*, *31*, *32*). Our observation of associated C and N anomalies establishes that IDPs contain heteroatomic organic compounds of presolar interstellar origin that are more complex than the simple deuterated compounds implied by earlier measurements (*7*). During its prebiotic period, Earth may have accreted as much as a centimeter of abiotic carbonaceous matter every million years, much of it settling to the surface within small (<25 μm diameter), high-surface-area IDPs (*33*–*35*). This constant flux of particulate organic matter continues to be delivered to the surfaces of terrestrial planets today and includes interstellar molecules such as those found in Benavente.

Gas-phase reactions are expected to produce C isotopic fractionations, but different processes produce fractionation effects in opposite directions (*1*, *36*–*38*). Thus, it has been suggested that the lack of C isotopic anomalies in IDPs is due to the existence of multiple reaction pathways that cancel out any anomalies produced (*1*, *38*). Others have suggested that isotopic fractionation in C is inhibited through the condensation of CO onto grain surfaces and its participation in grain chemistry (*2*, *5*). Our observation of a ^{13}C depletion associated with a ^{15}N enrichment in Benavente shows that C isotopic fractionation does occur and requires processes that can produce both effects in the same material.

Gas-phase ion-molecule reactions can enhance the ^{12}C/^{13}C ratios of organic species (*36*, *37*) to the level observed in Benavente, but whether these reactions also result in depleted ^{14}N/^{15}N ratios has not been studied. Low-temperature interstellar chemistry as the source of the ^{15}N enrichments seen in IDPs has only recently been investigated theoretically. A study of ion-molecule exchange reactions involving the most abundant N-bearing species in interstellar clouds (*9*) indicated a maximum enhancement in ^{15}N of +250‰. Another recent model, investigating NH_3 formation in dense molecular clouds, suggests a maximum enrichment of +800‰ (*10*). These models are consistent with the modest enrichment in ^{15}N seen in the bulk IDP but fall short of the values needed to account for the +1270‰ enrichment in ^{15}N observed in the anomalous region. Moreover, it is not clear whether ^{15}N-rich ammonia can pass on its anomalous N to the organic hosts thought to be responsible for N isotopic anomalies in IDPs. If future investigations of interstellar chemistry cannot account for the C and N isotopic fractionations observed in IDPs, circumstellar origins may need to be considered.

References and Notes

1. A. G. G. M. Tielens, in *Astrophysical Implications of the Laboratory Study of Presolar Materials*, T. J. Bernatowicz, E. Zinner, Eds. (AIP Conference Proceedings 402, American Institute of Physics, Woodbury, NY, 1998), pp. 523–544.
2. S. Messenger, R. M. Walker, in *Astrophysical Implications of the Laboratory Study of Presolar Materials*, T. J. Bernatowicz, E. Zinner, Eds. (AIP Conference Proceedings 402, American Institute of Physics, Woodbury, NY, 1998), pp. 545–564.
3. H/D = 6666, ^{12}C/^{13}C = 90, and ^{14}N/^{15}N = 272. Isotopic anomalies are often expressed as delta values, representing the deviation of the measured isotopic ratio from the terrestrial standard in parts per thousand (‰).
4. J. P. Bradley, in *Meteorites, Planets, and Comets*, A. M. Davis, Ed. (Vol. 1, Treatise on Geochemistry, H. D. Holland, K. K. Turekian, Exec. Eds., Elsevier Science, 2003), pp. 689–711.
5. S. Messenger, F. J. Stadermann, C. Floss, L. R. Nittler, S. Mukhopadhyay, *Space Sci. Rev.* **106**, 155 (2003).
6. T. J. Millar, A. Bennett, E. Herbst, *Astrophys. J.* **340**, 906 (1989).
7. S. Messenger, *Nature* **404**, 968 (2000).
8. C. M. O'D. Alexander *et al.*, *Meteorit. Planet. Sci.* **33**, 603 (1998).
9. R. Terzieva, E. Herbst, *Mon. Not. R. Astron. Soc.* **317**, 563 (2000).
10. S. B. Charnley, S. D. Rodgers, *Astrophys. J.* **569**, L133 (2002).
11. C. Floss, F. J. Stadermann, *Lunar Planet. Sci.* **33**, 1350 (2002).
12. C. Floss, F. J. Stadermann, *Lunar Planet. Sci.* **34**, 1238 (2003).
13. L. P. Keller, S. Messenger, M. Miller, K. L. Thomas, *Lunar Planet. Sci.* **28**, 707 (1997).
14. J. Aléon, F. Robert, M. Chaussidon, B. Marty, C. Engrand, *Lunar Planet. Sci.* **33**, 1397 (2002).
15. J. Aléon *et al.*, *Lunar Planet. Sci.* **34**, 1308 (2003).
16. Jacinto Benavente won the Nobel Prize for Literature in 1922 for his contributions to Spanish drama.
17. Materials and methods are available as supporting material on *Science* Online.
18. The image was divided into 94 randomly generated regions similar in size and shape to the anomalous

region, with analytical errors (1σ) of 4% or less for both $^{14}N/^{15}N$ and $^{12}C/^{13}C$.
19. While the anomalous regions in C and N have slightly different shapes, the differences are at the limit of the lateral resolution of these smoothed images and are, therefore, of limited importance. However, all extracted C and N isotopic ratios (e.g., Fig. 1) refer to identical regions of interest and are, thus, spatially correlated.
20. Th. Fouchet *et al*., *Icarus* **143**, 223 (2000).
21. K. Hashizume, M. Chaussidon, B. Marty, F. Robert, *Science* **290**, 1142 (2000).
22. T. Owen, P. R. Mahaffy, H. B. Nieman, S. Atreya, M. Wong, *Astrophys. J.* **553**, L77 (2001).
23. K. Hashizume, M. Chaussidon, B. Marty, K. Terada, *Astrophys. J.* **600**, 480 (2004).
24. J. Aléon, F. Robert, M. Chaussidon, B. Marty, *Geochim. Cosmochim. Acta* **67**, 3773 (2003).
25. M. N. Fomenkova, S. Chang, L. M. Mukhin, *Geochim. Cosmochim. Acta* **58**, 4503 (1994).
26. C. Arpigny *et al*., *Science* **301**, 1522 (2003).
27. P. J. Heaney, E. P. Vicenzi, L. A. Giannuzzi, K. J. T. Livi, *Am. Mineral.* **86**, 1094 (2001).
28. J. P. Bradley, *Science* **265**, 925 (1994).
29. P. Hoppe, S. Amari, E. Zinner, R. S. Lewis, *Geochim. Cosmochim. Acta* **59**, 4029 (1995).
30. L. P. Keller, S. Messenger, J. P. Bradley, *J. Geophys. Res.* **105**, 10397 (2000).
31. S. J. Clemett, C. R. Maechling, R. N. Zare, P. D. Swan, R. M. Walker, *Science* **262**, 721 (1993).
32. G. J. Flynn, L. P. Keller, D. Joswiak, D. E. Brownlee, *Lunar Planet. Sci.* **33**, 1320 (2002).
33. D. E. Brownlee, in *Analysis of Interplanetary Dust*, M. E. Zolensky, T. L. Wilson, F. Y. M. Rietmeijer, G. J. Flynn, Eds. (AIP Conference Proceedings 310, American Institute of Physics, Woodbury, NY, 1994), pp. 5–8.
34. D. E. Brownlee, D. J. Joswik, M. E. Kress, S. Taylor, J. Bradley, *Lunar Planet. Sci.* **33**, 1786 (2002).
35. J. P. Bradley, D. E. Brownlee, *Science* **231**, 1542 (1986).
36. W. D. Langer, T. E. Graedel, M. A. Frerking, P. B. Armentrout, *Astrophys. J.* **277**, 581 (1984).
37. W. D. Langer, T. E. Graedel, *Astrophys. J.* **69**, 241 (1989).
38. S. A. Sandford, M. P. Bernstein, J. P. Dworkin, *Meteorit. Planet. Sci.* **36**, 1117 (2001).
39. This work was supported by NASA grants NAG5-13467 to C.F., and NAG5-10623 and NAG5-10696 to J.B.. The work by J.B., Z.D., S.B., and G.G. was performed under the auspices of the U.S. Department of Energy, National Nuclear Security Administration by the University of California, Lawrence Livermore National Laboratory (LLNL) under contract No. W-7405-Eng-48. Department of Energy (DOE) contract DE-AC03-76SF00098 supported electron microscopy performed at the National Center for Electron Microscopy at Lawrence Berkeley National Laboratory (LBNL) and infrared spectroscopy performed at the Advanced Light Source (ALS) at LBNL. We thank T. Smolar of Washington University for NanoSIMS maintenance and support, M. Martin and ALS personnel for providing the ALS beamline, and K. Moore at LLNL for assistance with energy-filtered imaging.

Supporting Online Material
www.sciencemag.org/cgi/content/full/303/5662/1355/DC1
Materials and Methods
References

4 November 2003; accepted 26 January 2004

Legionella Effectors That Promote Nonlytic Release from Protozoa

John Chen,[1] Karim Suwwan de Felipe,[2] Margaret Clarke,[3] Hao Lu,[3] O. Roger Anderson,[4] Gil Segal,[5] Howard A. Shuman[1]*

***Legionella pneumophila*, the bacterial agent of legionnaires' disease, replicates intracellularly within a specialized vacuole of mammalian and protozoan host cells. Little is known about the specialized vacuole except that the Icm/Dot type IV secretion system is essential for its formation and maintenance. The *Legionella* genome database contains two open reading frames encoding polypeptides (LepA and LepB) with predicted coiled-coil regions and weak homology to SNAREs; these are delivered to host cells by an Icm/Dot–dependent mechanism. Analysis of mutant strains suggests that the Lep proteins may enable the *Legionella* to commandeer a protozoan exocytic pathway for dissemination of the pathogen.**

Several intracellular pathogens including *Legionella pneumophila*, *Mycobacterium avium* (*1*), *Chlamydia spp.* (*2*), and *Francisella tularensis* (*3*) are able to replicate within protozoan trophozoites. Thus, free-living amoebae may serve as a significant reservoir for pathogens in the environment, perhaps even as a "training environment" for the selection of virulence-related traits in these pathogens (*4*). *L. pneumophila*, the causative agent of legionnaires' disease, is frequently detected in association with *Hartmanella vermiformis* at the sources of infection during outbreaks (*5*). Under experimental conditions, *L. pneumophila* can multiply within and kill a variety of phylogenetically unrelated protozoa ranging from *Acanthamoeba castellani* to the genetically well characterized social amoeba *Dictyostelium discoideum* (*6*, *7*).

Intracellular pathogens have evolved three distinct strategies for surviving phagosome-lysosome fusion. Two of these mechanisms, tolerance of the toxic environment and escape from the phago-lysosome into the cytosol, are used by a variety of pathogens such as *Salmonella enterica* and *Listeria monocytogenes*, respectively. *L. pneumophila* and several other prokaryotic and eukaryotic intracellular pathogens use a third strategy—prevention of phagosome-lysosome fusion. After uptake of *L. pneumophila* by macrophages or protozoa, the bacteria are found within a specialized vacuole that does not fuse with lysosomes and does not acidify (*8*, *9*); this allows replication to proceed. The specialized vacuole associates with endoplasmic reticulum (ER)–derived secretory vesicles (*10*), mitochondria, and rough ER (*11*, *12*) and, near the end of the replicative cycle, acquires late endosomal markers (*13*). These observations strongly suggest that the bacteria play an active and continuous role in modulating organelle trafficking events from within the confines of their specialized vacuole.

A group of 24 genes called *icm* (intracellular multiplication) (*14*) or *dot* (defect in organelle trafficking) (*15*) are required for intracellular multiplication of *L. pneumophila*. Sequence similarity between several Icm/Dot proteins and those of the conjugative system of IncI plasmids colIb-9 and R64 (*16*) indicates that the Icm/Dot proteins form a type IV secretion system (TFSS) that delivers effectors to host cells. However, *L. pneumophila* mutants lacking the previously identified RalF or LidA effectors do not display obvious defects in organelle trafficking or intracellular replication (*17*, *18*). Because direct biochemical observation of infected cells has not led to the identification of additional effectors in *L. pneumophila*, we searched the genome sequence database for candidate genes.

As the modulation of organelle trafficking events appears to be important during intracellular multiplication, we looked for *L. pneumophila* effectors that resemble components of the SNARE system (*19*) and that might somehow disable or alter its function. Two such open reading frames (ORFs) were identified. Both exhibit limited sequence similarity to mammalian EEA1 and yeast USO1, proteins known to be involved in vesicle trafficking. Both *Legionella* ORFs are predicted to encode large regions of α-helical coiled-coils, structures present in EEA1 and USO1 and also commonly found in SNAREs (table S1).

As there are no functional assays for these putative effectors, we investigated whether *L.*

[1]Department of Microbiology, and [2]Integrated Program in Cellular, Molecular and Biophysical Studies, College of Physicians and Surgeons, Columbia University, 701 West 168th Street, New York, NY 10032, USA. [3]Program in Molecular and Cell Biology, Oklahoma Medical Research Foundation, 825 N.E. 13th Street, Oklahoma City, OK 73104–5046, USA. [4]Department of Biology, Lamont-Doherty Earth Observatory, Columbia University, 61 Route 9W, Palisades, NY 10964–1000, USA. [5]Department of Molecular Microbiology and Biotechnology, George S. Wise Faculty of Life Sciences, Tel-Aviv University, Ramat-Aviv, Tel-Aviv 69978, Israel.

*To whom correspondence should be addressed. E-mail: has7@columbia.edu